*Progress In Electromagnetics Research C, Vol. 26, 29–42, 2012*

# MATCHING NETWORK USING ONE CONTROL ELEMENT FOR WIDELY TUNABLE ANTENNAS

**C.-S. Lee and C.-L. Yang***

Department of Electrical Engineering, National Cheng Kung University, Tainan 70101, Taiwan

**Abstract**—A tunable impedance matching network is applied to achieve very widely tunable antennas, whose geometries are independent and unchanged to simplify the design. The attached matching network as the antenna feeding network enables any unspecified UWB antenna to tune the operation frequency continuously with high selectivity by merely one single control. This is quite different from filter-based concept which is complicated to co-design and implement a tiny narrow band tunable filter over wide frequency ranges and very difficult to control with one element. And also the design, adjustment, and optimization of the matching network are much simpler, quicker, and lower cost than geometry-modified antenna design. The analysis of precise high frequency circuit models is used predict the performance in simulation. Fabricated prototype antennas are measured by using horn antennas to validate the antenna performance. The tunable frequency ranges from 1.8 GHz to 2.8 GHz (155%) and 2.19 GHz to 3.86 GHz (176%). Moreover, compared to other matching network-based solutions, non-ideal effects in undesired bands other than the operation frequency band are suppressed, so the performance is improved. One wide-tuning antenna using one single element to control can be carried out by tunable matching networks without complicated designs.

## 1. INTRODUCTION

Impedance matching networks are widely implemented between radio transmitting, receiving systems and active microwave measurement circuits. The design of matching networks improves the performance of the antenna and the RF front-end in mobile terminals to maximize

*Received 20 October 2011, Accepted 30 November 2011, Scheduled 6 December 2011*

* Corresponding author: Chin-Lung Yang (cyang@mail.ncku.edu.tw).

the total system efficiency of the transmitter or receiver. We can use this characteristic to integrate various bands into one platform, so a single tunable antenna is desired to operate in adjustable bands. The aims of the tunable antennas over different bands are to improve the flexibility and selectivity of the operation bands and to lower the noise and interference. These tunable antennas can be carried out by different designs [1–6]. The tuning function can be achieved by modifying antenna geometries, the load reactance, and effective current paths to radiate and operate in different modes. Tunable effects can be fulfilled by the switches or varactors fabricated by the semiconductors or MEMS components. These techniques have challenges including limited tuning ranges, the complexity of the geometries, analytical principles, discrete tunable bands using switches, and the restriction of particular architectures.

A different concept is proposed for tunable antenna designs. In contrast to the viewpoint of using electro magnetics to design the radiator of the tunable antenna, a microwave circuit theory is adopted by designing a tunable microwave circuit at the antenna feeding port [7]. A simple tunable antenna based on impedance matching network circuit concept is designed as shown in Fig. 1. All we need is an arbitrary UWB antenna which inherently provides a large available bandwidth, implying a wide tuning range. Meanwhile, a tunable matching network can reconfigure the input impedance of the antenna at the desired operating frequencies with high selectivity to improve the signal to noise and interferences ratio (SINR). The design principle, analysis, and the fabrication are simple and flexible.

The concept is similar with the antenna with filters, but this architecture and analysis is quite different. A tunable filter provides an excellent selectivity on desired bands for a wideband antenna;

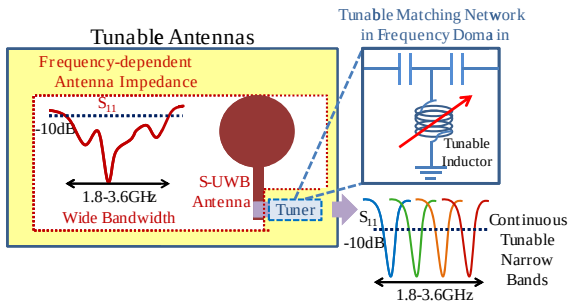


**Figure 1.** The proposed architecture of tunable antenna using matching network.

however, the tunable filters are usually difficult to design and control with just one single controllable element, especially for narrow band tunable filters over wide frequency ranges. Concerning the tunable frequency range, tunable filters with high selectivity usually come along with a limited tuning range and high complexity. Furthermore, there is another problem in the filter and antenna integration co-design. Normally, filters and antennas need co-design from an initial antenna geometric structure. Then filters are not simply connected directly with antennas, but they have to be re-designed as a compact frontend. Mostly the filters are complicated to adjust their implementation if the filters have a high order. Our proposed architecture uses only four lumped elements, which is independent of the original antenna prototype, and the antenna and the matching network can be designed separately. The comparison is listed in Table 1. Our proposed architecture has advantages of very wide tuning ranges, flexible control, and easy analytic models. The number of plus signs in the Table 1 represents the rank of complexity for each frequency tuning types. The more plus signs means easier control or lower system complexity to adjust frequency. Several types of frequency tuning functions are compared including general tunable antenna, tunable filter, and this work.

For the first one, the principles for the tunable filters have numerous and profound analysis theorems. Normally, the techniques need reconfigurable methods for feeding, the resonance frequency, the internal and external coupling intensity. All of these factors should be considered and designed at the same time, and these factors are not independent to design. In [8], reconfigurable filters with tunable and switchable impedance matching networks are more challenging to design than their fixed valued counterparts due to the requirements in pass-band impedance matching, stop-band rejection, and transitional performance. Switchable or tunable impedance matching networks utilize passive components with several discrete values to provide impedance matching at several frequencies with continuously adjustable or switchable values to achieve impedance

**Table 1.** Typical comparison for frequency tuning functions.

| **Tuning Types** | **Tuning** | | **Analysis** | **Impedance Matching** | **Antenna Patterns** |
|---|---|---|---|---|---|
| | **Range** | **Control** | | | |
| Modified Geometry | Broad | +++ | Middle | Yes | Yes |
| Tunable Filter | Narrow | + | Hard | No | No |
| **This Work** | **Very Wide** | ++++ | **Easy** | **Yes** | **No** |

matching. So tunable filter-based solutions are relatively complicated in control and design. Many fabrication technologies are available for a tunable RF impedance matching network [9]. In this paper, the proposed prototype is implemented with discrete SMD components to verify concepts, and these components can be further integrated on chip in compact size in the future.

The main design issues of tunable matching network include applicable frequency ranges, impedance tuner dynamic range, control methods, linearity, size and losses. The four main investigative objectives in this paper are operating frequency ranges, suppression of the other undesired bands, the use of one single tuning component, and energy loss reduction. The details of the design principles and the implementations of matching network will be presented in Section 2. In the Section 3, the measurement setup is illustrated and the results will be analyzed and summarized in Section 4. Finally, the conclusion will be drawn in Section 5.

## 2. ANALYSIS AND SIMULATIONS FOR TUNABLE MATCHING NETWORK

A complete impedance matching theory and numerical analysis are well-established [10–12]. In realistic operation, there exists a high complexity and practical performance loss after considering the parasitic effects, fabrication errors and self-resonant frequency of components, resulting in a frequency deviation away from the designed frequency. The $\pi$- and T-type networks themselves can be designed with a desired $Q$ value. However, one common problem for the wideband matching is that other undesired bands might happen to be matched unintentionally, especially for UWB antennas. Moreover, one drawback of using a varactor which needs an additional bias input results in discontinuity and parasitic effects from the biasing network. All of these factors above shall be taken into consideration seriously in this design topic to increase the selectivity performance. These practical factors are also taken into account for simulation, especially for the models of precise values in high frequency.

In contrast to L-type network which has limited matchable impedance ranges and lack of freedom for controllable $Q$ values, T-type and $\pi$-type networks are commonly confined to carry out high selectivity and a wide scope of tunable impedance dynamic ranges. A T-type (C-L-C) matching network is chosen and shown in Fig. 2. The central shunt part is the variable inductor $L$, implemented by a fixed $L$ and series a varactor.

Implementation is one of the major considerations to select the

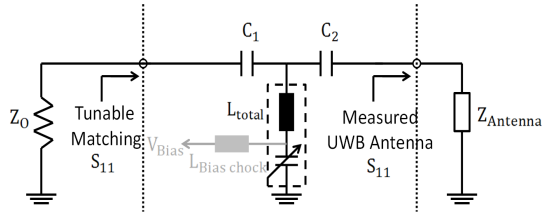


**Figure 2.** Equivalent circuit of the tunable matching network and UWB antenna with control voltages $V_{BIAS}$, series capacitor, shunt inductor $L$, and varactor.

proper architecture of the $\pi$- and T-type networks. In the RF circuit fabrication, shunt variable device is easier to implement. Also, low loss and ease control are desired, so only one variable shunt device in T-type network is what we choose. The design procedure and the principles to design in a simple structure and to determine the value of components, are presented as follows.

### 2.1. Analysis for High $Q$ Tunable Impedance Matching

Matching range is related to bandwidth of the UWB antennas, and one of the unique merits for UWB antennas is that the input impedance of an UWB antenna mostly resembles to $50\,\Omega$ overa very broad bandwidth.Based on this characteristic, we can simplify analysis that $50\,\Omega$ terminals are used at both ports of the matching network as the preliminary design to determine the values of $C_1$, $C_2$, and $L$, so the unknown variables significantly reduce.We can simplify design matching network by using two similar fixed low-value capacitors $C_1$ and $C_2$ for the two serial components. The results from implementation have proved that this nearly $50\,\Omega$ assumption does not affect the accuracy of the evaluation.

A graphical method of tracing the impedance trajectory is proposed to realize the selectivity. By using the right series capacitor $C_2$ (high capacitive reactance), the original antenna impedance, $Z_{ANT}$, will move to the right half of Smith chart ($Z_2$) along the unit circuit, and the end point intersects with high $Q$ circle. The trajectory is shown in Fig. 3. Therefore, *the target matching frequency is set by a 'single' variable inductor* $L$ and the impedance becomes $Z_1$. This enables a single control element design for tunable antenna. Then, by applying the up-down symmetrical nature of Smith chart,a left series capacitor $C_1$ of the same value ($C_1 = C_2 = C$) pulls impedance $Z_1$ back to the center point $Z_o = 50\,\Omega$. The tuning antenna is operated at this band thereby. As the large $C_1$ and $C_2$ are applied, a low selectivity can be

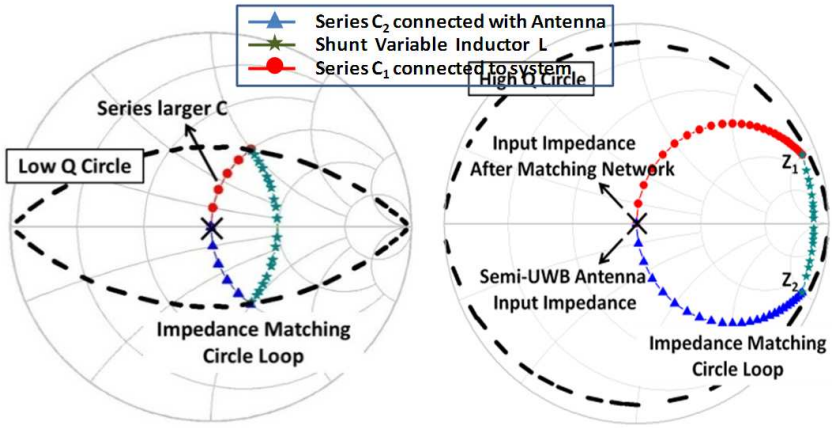


**Figure 3.** Matching analysis on Smith chart with (a) High $Q$. (b) Low $Q$ value.

fulfilled theoretically as shown in Fig. 3(b).

An analytic formula for calculating the unknown inductance can be established, so the unknown inductance value $L$ can be determined as a function of the tunable frequency. The impedance relationship of T-type (C-L-C) network is given as (1).

$$Z_{IN}(\omega) = \left( \left( Z_{Ant}(\omega) - \frac{j}{\omega C_2} \right)^{-1} - \frac{j}{\omega L_{total}} \right)^{-1} - \frac{j}{\omega C_1} \tag{1}$$

Applying the conditions of $Z_{ant} \cong Z_o$, $C_1 = C_2 = C$ (constant) to and the target frequency $\omega_{target}$ to simplify this equation, the Equation (3) is obtained to determine the inductor $L_{total}$.

$$f_{band,center} = \frac{\omega_{target}}{2\pi} = \frac{1}{2\pi} \times \sqrt{\frac{1}{(2LC - C^2 Z_o^2)}} \tag{2}$$

where $L_{total}$ is implemented by a fixed $L$ in series with a varactor which enables continuous tuning. Through thrureflect-line (TRL) calibration, the values of the capacitance, the inductance with the parasitics can be obtained precisely. Also, the actual values can be applied to achieve the predicted frequency and the precise frequency tuning ranges.

$$L_{total} \approx \frac{1}{2} \left( C Z_o^2 + 1 / \left( \omega_{taget}^2 \right) C \right) \tag{3}$$

After the theoretical matching inductance, $L_{total}$, and the corresponding cascaded capacitance, $C_{varactor}$, are calculated,the bias voltage value for the required capacitance can be determined from the measured $C$-$V$ curve of the varactor. Therefore, the variable inductor can be modeled with a proper varactor model which can be referenced in [13]. The varying range of the inductance is dominated by this varactor implying a practical limitation of the tuning range. This practical factor has thus determined the tunable ranges. In this paper, a preliminary validation up to 4 GHz is verified. The components are not optimized intentionally yet.

Beside, due to the SMD component tolerance errors, the actual implemented operation frequency might be deviated. The precise operation frequency can be obtained by calibrating the actual RF inductance models and correcting the bias voltage slightly for precise capacitance.

## 2.2. Controllable Bandwidth

The selectivity in our proposed architecture can be determined by the pre-selection of the $C_1$ and $C_2$ values. We can estimate the bandwidth by circuit $Q$ values. We set a redundant resistance ($R_V$) as the mediate step to design matching network. T-type matching network is regarded as two cascaded L-shaped networks. The relationship is shown below.

$$Q_1 = \sqrt{\frac{R_V}{R_S} - 1}, \quad Q_2 = \sqrt{\frac{R_V}{R_L} - 1} \tag{4}$$

The unloaded $Q$ of the cascaded network $Q \fallingdotseq \max(|Q_1|, |Q_2|)$, and the BW can be determined by $2/|Q|$. Also, from the previous analysis of (3), if we choose a small capacitance $C$, high $Q$ will be achieved and the bandwidth is narrow; meanwhile, the tuning ranging is smaller. This can be observed from (3). The range of the $L_{total}$ is limited by the chosen varactor. As the $C$ values decreases, the $\omega_{target}$ can have small variation range or the covered tunable frequency will be smaller. In [14], the constraints from the quality factor are investigated. Fig. 4 shows that a controllable bandwidth study is demonstrated in simulation.The central frequency is fixed at 2.4 GHz, and three $Q$ values can be designed by setting $C$ = 0.3, 0.75, and 1.2 pF. The controlled bandwidths are 60 MHz, 125 MHz, and 230 MHz (2.5%, 5.2%, and 9.6%), respectively. In this paper, the middle $Q$ case is selected to implement for test.

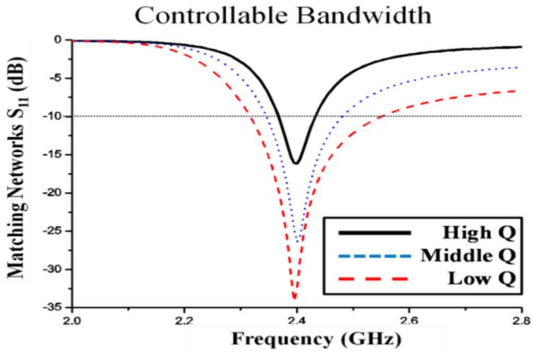


**Figure 4.** Comparison of different bandwidths. The $S_{11}$ results of simulated match networks of high, middle, and low $Q$ cases using $C = 0.3$, 0.75, and 1.2 pF, respectively, with port 1 and port 2 both connected to 50 Ω.

### 2.3. Impacts of Initial Phase on Transducer Power Gain

There exists a definite loss in passive matching network itself. The insertion loss is mainly influenced by the tunable network topology. Both T-type and $\pi$-type topologies have the features of mirror-inverted characteristics. However, how the variable device series or shunt combine together in hybrid type matching network circuit structure, these two type have shown different transducer power gain, $G_T$, towards different load impedances [9], which is defined as Equation (5) and is regarded as a better parameter to quantify insertion loss.

$$G_T = 10 \log \frac{|S_{21}|^2}{1 - |S_{11}|^2} \tag{5}$$

The transducer gain is found to be related to the initial impedance, so we control this factor on purpose to achieve high $G_T$. By shifting the initial impedance phase the insertion loss can be alleviated. Some of the UWB antenna impedances may be relatively low impedance, and these will affect $G_T$ values of T-type matching network to be low. In [10], we understand that T-type topologies, for tunable shunt reactance parts are suitable for high impedance matching. Therefore, the better range for T-type matching is at the right half plane of Smith chart. Based on the measurement results of the original UWB antenna in Fig. 5(a), the input impedance in the target frequency ($1.8 \sim 2.6$ GHz) is mainly located on the left side of the Smith chart, causing a slightly poor transducer gain at this range. To further improve the $Q$ value, an extra transmission line is re-designed in front

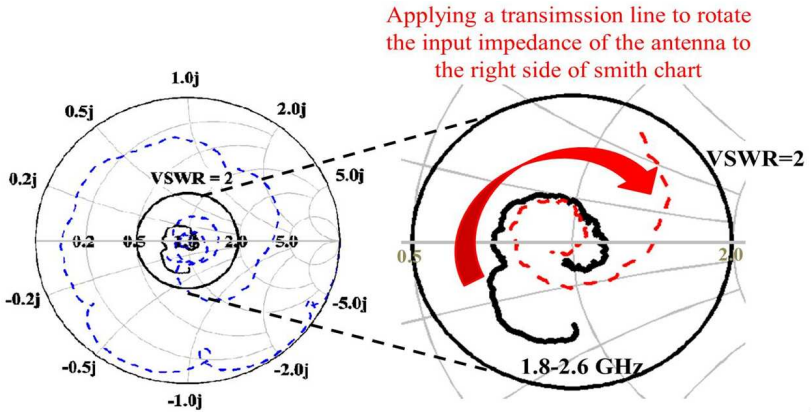


(a) (b)

**Figure 5.** (a) Measured UWB antenna impedance of 300 MHz $\sim$ 6 GHz. The impedances in desired bands (solid line) in the circle of VSWR = 2 are shown. (b) Rotate initial phase (1.8 $\sim$ 2.6 GHz) to the right side of Smith chart plane.

of matching network, so the impedance in the desired frequency band changes to right part in Smith chart, as shown in Fig. 5(b).

## 3. FABRICATION AND MEASUREMENTS SETUP

To implement the proposed wide tuning antenna, three major parts are fabricated including an UWB antenna, a tunable matching network, and a controlling circuit. The UWB antenna is fabricated without fully optimized performance. A circular-shaped antenna is chosen as a simple design on FR4 ($\varepsilon_r = 4.3$, loss tangent $\delta = 0.015$, thickness of 1.6 mm). The relevant dimensions of antenna are $[r/d/g/w_f]$ = 21.3/1/10/2.7 mm and $[L_1/L_2/W] = 62/19/64$ mm. The dimension is shown in Fig. 6.

The whole fabricated tunable antenna is shown in Fig. 7, including the matching network on Roger R04003C substrate ($\varepsilon_r = 3.55$, loss $\tan\delta = 0.0021$, thickness = 32 mil (0.81 mm)). The component values are $C_1 = C_2 = 0.6$ pF, $L_2 = 4.7$ nH, and $L_{Biaschoke} = 7.8$ nH (for control voltage input). The GaAshyperabrupt (MGV-125-23-E28) varactor with the $Q$ of 3000 is tunable from 0.3 pF to 4 pF, and its series resistance is about 1 $\Omega$. The controlled circuitry is made by the micro-processor 89C51 to set a proper bias voltage on the varactor through a DAC and an OP-Amplifier, andthis control module can be miniaturized by using ASIC. The $S_{11}$ of the tunable antenna is

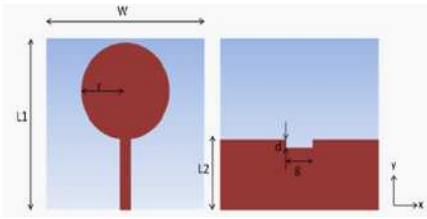


**Figure 6.** The geometry of UWB antenna.

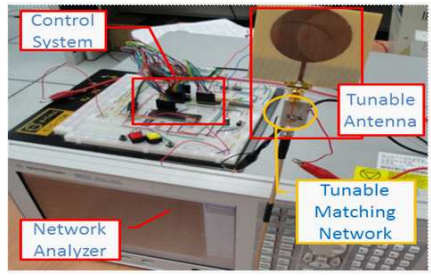


**Figure 7.** The implemented tunable UWB antenna attached with matching network.

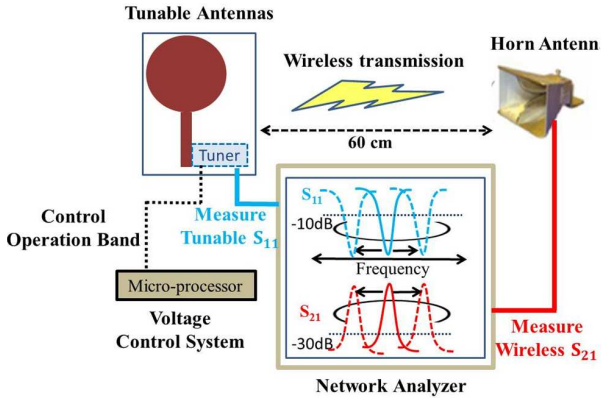


**Figure 8.** The whole measurement setup.

measured with the network analyzer Agilent N9020A. A double ridged UWB horn antenna ($1 \sim 18$ GHz) is placed at a distance of 60 cm in the far field to test the reception performance ($S_{21}$) of the antenna.

Figure 8 is the block diagram of whole measurement set-up. We design T-type matching network at antenna feeding point to tune the UWB antenna reflection coefficient for selectivity over different bands, and the performance is measured by E5071C network analyzer. A micro-processor is used to bias voltage to control tunable inductance value in the matching network. And additional transmitted horn antenna is attached to test the wireless transmission performance of the fabricated tunable antenna by recording the corresponding transmission coefficient $S_{21}$.

## 4. RESULTS AND DISCUSSIONS

An UWB horn antenna was used to compare wireless $S_{21}$ towards the UWB antenna itself with and without the frequency tunable matching network, corresponding to the wideband and narrow band reception, respectively. First, the frequency tuning capability of the proposed antenna is verified and only a single controlling voltage is applied. The measured $S_{11}$ results are shown in Fig. 9. The components are $C_1 = C_2 = 0.6\,\text{pF}$ with two different shunt inductances (a) 4.7 nH and (b) 2 nH. The varactor is biased from $0 \sim 23\,\text{V}$. These tunable bands cover two different ranges, 1.8–2.8 GHz (155%) and 2.19–3.86 GHz (176%), respectively.

The matching network can change the original UWB frequency response to the narrow band operation at the desired frequency, so this modified UWB antenna is validated as the novel tunable antenna

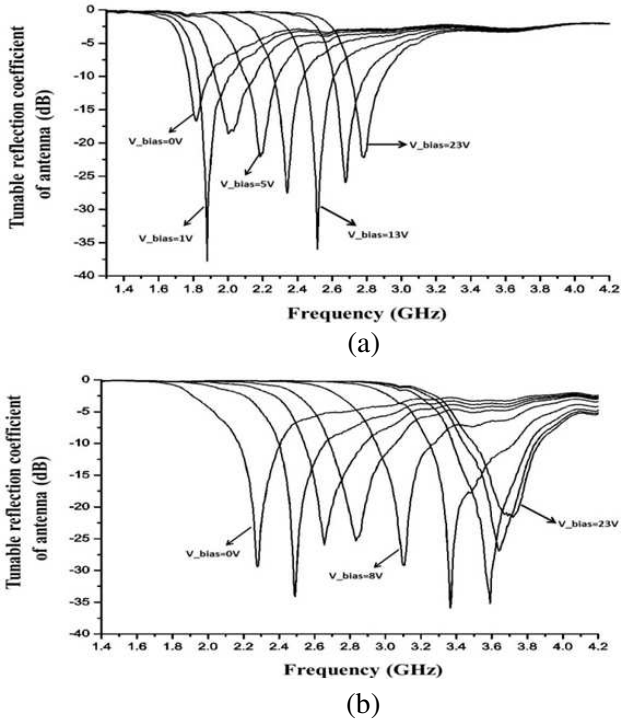


**Figure 9.** Measured results of tunable antenna reflection coefficientwith biased voltage from $0 \sim 23\,\text{V}$; $C_1 = C_2 = 0.6\,\text{pF}$; (a) $L = 4.7\,\text{nH}$; (b) $L = 2\,\text{nH}$.

**Table 2.** Performance of the tunable antenna with $C_1/L/C_2 = 0.6\,\text{pF}/2\,\text{nH}/0.6\,\text{pF}$.

| $V_{bias}$ (volts) | | 1 | 2 | 5 | 10 | 15 | 23 |
|---|---|---|---|---|---|---|---|
| Frequency (GHz) | 2.19 | 2.31 | 2.78 | 2.97 | 3.44 | 3.73 | 3.86 |
| Return Loss (dB) | −21.9 | −30.3 | −34.9 | −38.2 | −42.3 | −20.7 | −23 |
| $G_T$ (dB) | −0.94 | −0.93 | −0.89 | −0.82 | −0.7 | −0.61 | −0.58 |
| BW (MHz) | 288 | 240 | 239 | 300 | 432 | 324 | 222 |

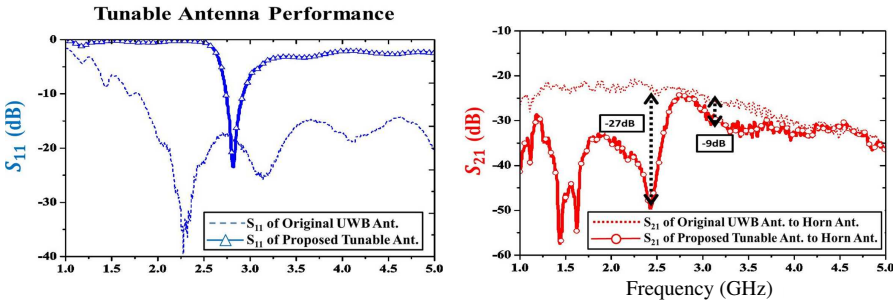


**Figure 10.** The reception performance of tunable antenna (a) $S_{11}$ and (b) $S_{21}$ with horn antenna in comparison with original UWB antenna.

by using the tunable matching network. Moreover, our results show that only one desired band can be matched without other undesired matched bands and that ensures quality selectivity. The performance of the tunable antenna can be listed in Table 2. This table shows the tunable range from 2.19 GHz to 3.86 GHz. The transducer power gain can be as low as −0.58 (up to −0.94 dB), which implies very low insertion loss.

Finally, the transmission performance is tested using an UWB horn antenna to the UWB antenna whose matching network is $C_1 = C_2 = 0.5\,\text{pF}$ and $L = 3\,\text{nH}$. The original performance ($S_{11}$ in Fig. 10(a) and $S_{21}$ in Fig. 10(b)) of the horn antenna to the UWB antenna are those two middle dashed lines shown in Fig. 10, and no selection capability is provided. The measured results from UWB antenna with the tunable matching network are the solid lines in the Figs. 10(a) and (b) and has shown an average bandwidth of around 300 MHz with tunable operating frequency band over $2.1 \sim 3.63$ GHz. The SINR can be improved by $\sim$ 10.67 dB due to the suppression in noises and interferences and low insertion loss in signals. The noise

power is estimated from the reduction of the bandwidth according to relationship of $P_N = \text{kTB}$, where the bandwidth is reduced from 3.2 GHz to 240 MHz ($1/13.3 = -11.25\,\text{dB}$), so the overall gain is 10.67 ($= 11.25 - 0.58$). Observing the adjacent bands next to target frequencies (2.83 GHz), left and right bands can be suppressed by $-27$ and $-9\,\text{dB}$, respectively. Furthermore, we would like to point out that most of the matching network on wideband impedance happens to have the phenomenon that multiple undesired bands may be matched, but in our design, only one target band is matched and other unintended bands are all suppressed. Compared with the original UWB antenna, the selectivity had been upgraded significantly with only slight energy loss.

## 5. CONCLUSION

In this paper, we apply a tunable matching network to fulfill ultra-wide tuning range antennas and have succeeded in verifying its high selectivity, wide tuning range and low loss. The measurement results show that the matching network controlled by only one single bias voltage features an average transducer power gain of $-0.58 \sim -0.94\,\text{dB}$ and enables the tunable ratio of 176%. All these results recommend that this proposed concept can lower the process, time and analytical difficulty of the traditional tunable antenna design significantly. In the future, this design concept can be applied in designing and controlling multi-band tunable antennas as well.

## REFERENCES

1. Nguyen, V.-A., M. T. Dao, Y. T. Lim, and S. O. Park, "A compact tunable internal antenna for personal communication handsets," *IEEE Antennas Wireless Propagat. Lett.*, Vol. 7, 2008.
2. Melde, K. L., H.-J. Park, H.-H. Yeh, B. Fankem, Z. Zhou, and W. R. Eisenstadt, "Software defined match control circuit integrated with a planar inverted-F antenna," *IEEE Trans. on Antennas and Propagation*, Vol. 58, 3884–3890, 2010.
3. Sheta, A.-F. and S. F. Mahmoud, "A widely tunable compact patch antenna," *IEEE Antennas Wireless Propagat. Lett.*, Vol. 7, 40–42, 2008.
4. Hai, J., M. Patterson, C. Zhang, and G. Subramanyam, "Frequency tunable microstrip patch antenna using ferroelectric thin film varactor," *Aerospace & Electronics Conference (NAECON), Proceedings of the IEEE 2009 National*, 248–250, 2009.

5. Yang, S.-L. S., A. A. Kishk, and K.-F. Lee, "Frequency reconfigurable U-slot microstrip patch antenna," *IEEE Antennas Wireless Propagat. Lett.*, 127–129, Vol. 7, 2008.
6. Nikolaou, S., R. Bairavasubramanian, C. Lugo, Jr., I. Carrasquillo, D. C. Thompson, G. E. Ponchak, J. Papapolymerou, and M. M. Tentzeris, "Pattern and frequency reconfigurable annular slot antenna using PIN diodes," *IEEE Trans. on Antennas and Propagation*, Vol. 54, No. 2, 439–448, Feb. 2006.
7. Yang, C.-L., "Novel high selective band-tunable antennas over ultra-wide ranges using reconfigurable matching network," *IEEE Antennas and Propagation Society International Symposium*, 1–4, Jun. 2009.
8. Nieuwoudt, A., J. Kawa, and Y. Massoud, "Automated design of tunable impedance matching networks for reconfigurable wireless applications," *45th ACM/IEEE Design Automation Conference*, 498–503, 2008.
9. Hoarau, C., N. Corrao, J.-D. Arnould, P. Ferrari, and P. Xavier, "Complete design and measurement methodology for a tunable RF impedance-matching network," *IEEE Trans. on Microwave Theory and Techniques*, Vol. 56, No. 11, 2620–2627, Nov. 2008.
10. Schmidt, M., E. Lourandakis, A. Leidl, S. Seitz, and R. Weigel, "A comparison of tunable ferroelectric PI and T-matching networks," *Proceedings of the 37th European Microwave Conference*, 98–101, 2007.
11. Thompson, M. and J. K. Fidler, "Determination of the impedance matching domain of passive LC ladder networks: Theory and implementation," *J. Franklin Institute*, Vol. 333(B), No. 2, 141–155, 1996.
12. Sun, Y. and J. K. Fidler, "Design method for impedance matching networks," *IEE Proceedings Circuits, Devices and Systems*, Vol. 143, 186–194, 1996.
13. Stauffer, G. H., "Finding the lumped element varactor diode model," *High Frequency Electronics*, Summit Technical Media, 2003.
14. Yuliang, Z., H. Maune, A. Giere, M. Sazegar, and R. Jakoby, "Constraints on efficient control of tunable impedance matching network based on barium-strontium-titanate thick-film varactors," *38th European Microwave Conference*, 805–808, 2008.